Research Article

Jun Yuan, Rongpeng Liu, Shasha Sheng, Haihui Fu*, Xiaoyun Wang*

Integrated metabolomic and transcriptomic profiling revealed coping mechanisms of the edible and medicinal homologous plant *Plantago asiatica* L. cadmium resistance

https://doi.org/10.1515/biol-2022-0501
received June 09, 2022; accepted August 25, 2022

Abstract: Rapidly increasing cadmium (Cd) pollution led to the increase in contamination in farmland. The study explained the Cd resistance mechanisms of *Plantago asiatica* L. via physiological, metabolomic, and transcriptomic analyses. The results showed that as soil Cd level increased, proline content declined and then increased significantly. In contrast to the H_2O_2 content change trend, contents of soluble protein and malondialdehyde (MDA) first decreased, then increased, and finally, declined. Leaf Cd concentration was positively related to soluble protein content and negatively to both MDA content and activities of superoxide dismutase (SOD) and catalase (CAT). Most of the top 50 differential metabolites belonged to organic acids and sugars. Besides combining metabolome and transcriptome data, in the metabolic network involving the target metabolic pathways (e.g., ascorbate and aldarate metabolism, glutathione metabolism, galactose metabolism, and glyoxylate and dicarboxylate metabolism), dehydroascorbate (DHA), regulated by L-ascorbate peroxidase (APX) and L-gulonolactone oxidase (GULO), was significantly up-regulated. This illuminated that, in *P. asiatica*, CAT and SOD played vital roles in Cd resistance, and soluble protein and MDA acted as the main indexes to characterize Cd damage. It also suggested that DHA functioned effectively in Cd resistance, and the function was regulated by APX and GULO.

Keywords: Cd stress, differential metabolites, differentially expressed genes, physiologies, *Plantago asiatica* L.

1 Introduction

Plantago asiatica, a common medicinal and edible plant, is native to China, Japan, and Korea [1]. *P. asiatica* contains many natural active ingredients (e.g., plantamajoside, flavonoids, tannins, iridoids, and sterols) and has been widely used as traditional medicine and dietary health supplement for more than 2,000 years in Eastern Asia [2]. Due to abundant resources and low price, it has been widely used in the treatment of many diseases (e.g., infectious diseases, skin diseases, and problems concerning the digestive organs, respiratory organs, reproduction, and the circulation for the various pharmacological effects; e.g., wound healing, antidiarrheal, and anti-inflammatory) [3]. Several researches on the chemical constituents and physiological activities of *P. asiatica* have laid down the theoretical foundations for the development of *P. asiatica* safety research [4–6].

The safe use of traditional plant medicine has attracted a lot of attention [7], when heavy metals (especially cadmium [Cd]) exceed the standard in commercially available medicinal materials [8–10]. Cd has the characteristics of high bioaccumulation, strong bioavailability, and high biotoxicity, and it easily migrates from soil to plants [11–13]. Eventually, Cd seriously threatens people's health through food chains [14]. Hence, much attention has been put to potential soil Cd contamination during the cultivation of medicinal plants [15,16].

* **Corresponding author: Haihui Fu,** Key Laboratory of Crop Physiology, Ecology and Genetic Breeding, Ministry of Education, Jiangxi Agricultural University, Nanchang 330045, China, e-mail: fhh819@163.com
* **Corresponding author: Xiaoyun Wang,** Research Center for Traditional Chinese Medicine Resources and Ethnic Minority Medicine, Jiangxi University of Chinese Medicine, Nanchang 330004, China, e-mail: wxy20052002@aliyun.com
Jun Yuan: School of Nursing, Jiangxi University of Chinese Medicine, Nanchang 330004, China
Rongpeng Liu: School of Pharmacy, Jiangxi University of Chinese Medicine, Nanchang 330004, China
Shasha Sheng: Research Center for Traditional Chinese Medicine Resources and Ethnic Minority Medicine, Jiangxi University of Chinese Medicine, Nanchang 330004, China

P. asiatica possesses the characteristic of fast growth and large biomass [3]. It has the ability to absorb and accumulate heavy metals and, thus, has soil remediation potential [17]. Heavy metals (e.g., Cd, Pb, and Cu) could accumulate in *P. asiatica*, destroy the membrane system, and inhibit leaf growth [17,18]. Because of the medicinal and edible value of *P. asiatica* and the toxic effects of Cd, it is of great importance to study the molecular mechanisms of heavy metal resistance of *P. asiatica*. In this study, taking *P. asiatica* under different levels of Cd stress as the sample, physiological, metabolomic, and transcriptomic analyses were conducted in a pot experiment. The main queries to be addressed are: (1) what are the main changes of *P. asiatica* in response to Cd at the metabolomic level? (2) what are the molecular mechanisms of *P. asiatica* Cd resistance based on transcriptomics and metabolomics? The study will help to understand how *P. asiatica* resists to Cd physiologically, metabolically, and transcriptionally.

2 Materials and methods

2.1 Plant materials

Topsoil (0–20 cm) was collected from Shennong garden of Jiangxi University of Chinese Medicine (JXUCM) in Nanchang City, Jinagxi Province, China, and sieved to remove stones. The soil properties were as follows: total N, 0.30 g/kg; total P, 0.28 g/kg; total K, 27.15 g/kg; available N, 0.01 g/kg; available P, 0.01 g/kg; available K, 0.08 g/kg; organic matter, 1.97 g/kg; pH, 4.6; total Cd, 0.92 mg/kg. The total Cd content in soil was lower than 1.0 mg/kg, which was the critical value of Cd ensuring the normal growth of plants.

The chemical reagent Cd chloride hemi (pentahydrate) ($CdCl_2{\cdot}2.5H_2O$) was added to the soil, obtaining 3, 10, 50, and 100 mg/kg Cd-treated soil according to Liu et al. [17] and Gong et al. [19]. The Cd-treated soil samples were aged for 30 days prior to the experiment. The treatments with different levels of Cd were named CK (0 mg/kg), T1 (3 mg/kg), T2 (10 mg/kg), T3 (50 mg/kg), and T4 (100 mg/kg).

P. asiatica seeds were selected from *P. asiatica* experiment plots in Xingan County of Jiangxi Province, China, and cultivated for about 5 months. It was identified as *P. asiatica* by Associate Prof. Xiaoyun Wang from JXUCM. The healthy and disease-free seedlings with uniform growth vigor were selected and transplanted into a flower pot (16 cm × 17 cm) with 2 kg unpolluted or Cd-treated soils, and each pot included one seedling. Each treatment included three repetitions, and each repetition included three seedlings. The plant leaves were harvested after 15 days. Sections of plant samples in all groups were dried at 65°C for 48 h to determine the Cd concentration, and other sections of the samples in CK and T3 were quickly frozen with liquid nitrogen and stored at −80°C for further physiological, metabolomic, and transcriptomic analyses.

2.2 Physiological analysis

The ninhydrin colorimetry was carried out to analyze the proline content. A 0.05 g fresh leaf was mixed with 5 mL of 3% sulfosalicylic acid in a centrifugal tube and extracted in the boiling water bath for 10 min. After cooling to room temperature, the extracted solution was filtered and diluted with distilled water to a volume of 25 mL. 2 mL of diluent was mixed with glacial acetic acid (2 mL) and acidic ninhydrin (2 mL) and then treated with a boiling water bath for 30 min. After cooling down, 4 mL of toluene was added, and they were shaken thoroughly until stratified during standing, followed by isolation of the upper layer to measure the absorbance at 520 nm with the ultraviolet spectrophotometer (UV-8000, Metash, China).

The Coomassie brilliant blue G-250 was used to detect the contents of soluble protein [20]. 0.05 g of fresh leaf was homogenized with 2 mL of water and then centrifuged at 4,000 rpm for 20 min. 0.1 mL of supernatants and 5 mL of G-250 reagent were mixed well and stood for 10 min, followed by isolation of the supernatant to measure the absorbance at 595 nm using the ultraviolet spectrophotometer.

Contents of malondialdehyde (MDA) and H_2O_2 were determined by assay kits (Suzhou Keming, China). 0.10 g of fresh leaf sample and 1 mL of solution (1:10, v/v) were homogenized in an ice bath and centrifuged at 4°C for 10 min. According to the instructions of the manufacturer, supernatant absorbances were detected at 532 and 600 nm to assess the MDA content and at 415 nm to assess the H_2O_2 content.

2.3 Extraction, derivation, and analysis of metabolites

Metabolite profiling analysis was conducted by gas chromatography-mass spectrometry (GC-MS; 7890A, Agilent,

USA) as described in the unpublished work. A total of 50 mg of fresh leaf samples were put into a 2.0 mL EP tube with 500 µL of methanol-chloroform (3/1, v/v) and 10.0 µL of ribitol and given a vortex for 30 s. After ground at 45.0 Hz for 4 min and underwent ultrasound exposure for 5 min in ice water bath, the mixture was centrifuged at 1,200 rpm for 15 min. A total of 300 µL of the supernatant were collected independently into 1.5 mL EP tube and dried in a vacuum concentrator (LNG-T98, Taicang City, China), until the upper polar phase was thoroughly dried. Then, methoximation, i.e. incubating the dried fraction at 80°C for 30 min with 60 µL of 20 mg/mL methoxyamine hydrochloride, and trimethylsilylation, i.e. incubating the dried fraction at 70°C for 1.5 h with 70.0 µL BSTFA (BSTFA:TMCS = 99:1, v/v), were sequentially performed. Once cooled to room temperature, 5 µL of FAMEs (dissolved in chloroform) were added in the mixture for further study.

The GC–MS analysis was conducted according to Yuan et al. [21]. In brief, 1 µL of samples were injected into a DB-5MS capillary column (30 m × 250 µm × 0.25 µm) (Agilent JW Scientific, Folsom, CA, USA). Following a solvent delay of 1 min, the GC oven temperature was adjusted to 50°C, and after injection for 1 min, the temperature was raised from 50 to 310°C at 10°C/min for 8 min. The temperature of ion source and front injector were adjusted to 250 and 280°C, respectively. Helium was used as the carrier gas at a constant rate of 3.0 mL/min. Determination was achieved with a mass range of 50–500 m/z and an electron impact at 70 eV.

The metabolite levels were detected by ChromaTOF (version 4.3X, Leco Corporation, MI, USA) with LECO-Fiehn Rtx5 database. The raw files were converted to NetCDF format and then processed by ChromaTOF to correct the baseline, search peaks, deconvolute spectrum, and align compounds of samples. Qualitative analysis of substances was performed by LECO-Fiehn Rtx5 database, including the matching of mass spectral and retention time index. Briefly, the data with no definite substance name or no spectrum comparison similarity were removed, metabolites of more than 50% missing in comparisons were removed, and metabolites of less than 50% missing were underwent the missing value imputation using the k-nearest neighbor algorithm. The metabolites were expressed in the peak area and normalized to the area of the internal standard (ribitol) for further analysis. A total of 185 peaks of the original data were retained.

2.4 Total RNA extraction and transcriptome sequencing

Total RNA extraction and transcriptome sequencing were conducted based on the unpublished work [22]. The total RNA was extracted using RNAprep Pure Plant Plus Kit (Tiangen Biotech, Beijing, China, DP441). RNA purity check, RNA concentration measurement, and RNA integrity assessment were performed using the Nano Photometer® spectrophotometer (IMPLEN, CA, USA), Qubit® RNA Assay Kit in Qubit® 2.0 Flurometer (Life Technologies, CA, USA), and RNA Nano 6000 Assay Kit of the Agilent Bioanalyzer 2100 system (Agilent Technologies, CA, USA), respectively.

A 3 µg RNA of each sample was used as input material for the RNA sample preparations. Sequencing libraries were constructed by NEBNext® Ultra™ RNA Library Prep Kit for Illumina® (NEB, USA). Briefly, mRNA was purified from total RNA using poly-T oligo-attached magnetic beads. Fragmentation was performed using divalent cations in NEBNext First-Strand Synthesis Reaction Buffer (5×). First-strand cDNA was synthesized with random hexamer primer and M-MuLV Reverse Transcriptase (RNase H-). Second-strand cDNA synthesis was subsequently conducted by DNA Polymerase I and RNase H. Remaining overhangs were converted into blunt ends via exonuclease/polymerase activities. After adenylation of DNA fragment 3′ ends, NEBNext Adaptor with hairpin loop structure were ligated to prepare for hybridization. The library fragments were purified with AMPure XP system (Beckman Coulter, Beverly, USA) to select the cDNA fragments of preferentially 150–200 bp in length. Then, 3 µL of USER Enzyme (NEB, USA) was applied with size-selected, adaptor-ligated cDNA at 37°C for 15 min followed by 5 min at 95°C before PCR. Then, PCR was conducted with Phusion High-Fidelity DNA polymerase, Universal PCR primers, and Index (X) Primer. Finally, PCR products were purified with AMPure XP system and library quality was assessed by the Agilent Bioanalyzer 2100 system.

The index-coded samples clustering was conducted on a cBot Cluster Generation System by TruSeq PE Cluster Kit v3-cBot-HS (Illumia). After cluster generation, the library preparations were sequenced on an Illumina Nova seq6000 platform and paired-end reads were generated.

Raw data (raw reads) of fastq format were processed through in-house perl scripts. Clean data (clean reads) were obtained by removing reads containing adapter or ploy-N and reads of low quality from raw data. Simultaneously, Q20, Q30, GC content, and sequence

duplication level of the clean data were calculated. All the downstream analyses were carried out based on the clean data of high quality.

2.5 Data analysis

First, analysis of variance [23] was performed to calculate the differences in Cd concentration, contents of soluble protein, MDA, proline, H_2O_2, and metabolites in different groups using SPSS 18.0 (SPSS Inc., USA). Pearson correlation analysis was carried out to estimate the relationships between leaf Cd concentration and soil Cd concentration and among Cd concentration, relative content of dehydroascorbate (DHA), contents of soluble protein, MDA, proline, H_2O_2 and GSH, and activities of superoxide dismutase (SOD), POD, and CAT in leaves. And the content of GSH and activities of SOD, POD and catalase (CAT) were showed in our unpublished work (Figure S2).

Second, the principal component analysis (PCA) was utilized to reveal the overall distribution of samples in CK and T3. The orthogonal partial least squares discrimination analysis (OPLS-DA) was conducted to assess differences of metabolite profiles in leaves between CK and T3. The OPLS-DA model was validated by permutation tests (200), and a $Q2$ value of above 0.5 and an $R2$ value of above 0.7 denoted that the model was highly significant. The variable importance in projection (VIP) values of metabolites was obtained from the OPLS-DA model. Metabolites with VIP of above 1.0 and p value of below 0.05 were selected as differential metabolites (DMs) [24], playing larger roles in distinguishing leaves in CK and T3. PCA and OPLS-DA analysis were performed using SIMCA-P version 14.1 (Umetrics, Sweden). Top 50 DMs were selected from the total DMs based on VIP values. According to the kyoto encyclopedia of genes and genomes (KEGG) pathway analysis of the top 50 DMs, target metabolic pathways were selected with $p < 0.05$.

Third, transcriptome assembly was accomplished using Trinity with min_kmer_cov set to 2 by default and all other parameters set default [24]. Gene function was annotated based on Nr (NCBI non-redundant protein sequences), Nt (NCBI non-redundant nucleotide sequences), Pfam (Protein family), KOG/COG (Clusters of Orthologous Groups of proteins), Swiss-Prot (Amanually annotated and reviewed protein sequence database), KO (KEGG Ortholog database), and GO (Gene Ontology). Gene expression levels were estimated by RSEM for each sample [25]. Differentially expressed genes (DEGs) between CK and T3 were selected using the DESeq R package (1.10.1). DESeq provides statistical routines for determining differential expression in digital gene expression data using a model based on the negative binomial distribution. The resulting p values were adjusted using the Benjamini and Hochberg's approach for controlling the false discovery rate. Genes with an adjusted $p < 0.05$ and fold change (ratio of expression between CK and T3) ≥ 2 or ≤ 0.5 were assigned as differentially expressed. Top 50 and top 200 DEGs were selected from the total DEGs based on the p-values.

Finally, KEGG pathway analysis was conducted with DMs and DEGs using MetaboAnalyst 5.0 and KOBAS software, respectively [21,26]. Spearman correlation between the top 50 DEGs and top 50 DMs was calculated using the psych package in R (V3.6.2) [27]. DEGs and DMs were labeled on the KEGG pathway map: upregulation was indicated in red, downregulation in green, and both upregulation and downregulation in blue. Correlation clustering heat map was drawn using the heatmap package with hierarchical cluster. Based on top 50 DMs and top 200 DEGs in KEGG pathway analysis, common pathways of the two analysis results were screened in a metabolic network.

3 Results

3.1 Physiological and biochemical characteristics in Cd-treated *P. asiatica*

The Cd concentration in leaves increased significantly with soil Cd level increasing ($p < 0.05$) (Figure 1). As soil Cd level increased, proline content decreased and then increased significantly ($p < 0.05$), contents of soluble protein and MDA first decreased and then increased and eventually decreased significantly ($p < 0.05$). Conversely, H_2O_2 content increased, then declined, and finally, increased significantly ($p < 0.05$) (Figure 2). Compared to CK, contents of proline, MDA and H_2O_2 in T3 were reduced 29, 68, and 6%, respectively, and contents of soluble protein in T3 were increased by 0.85 times (Figure 2).

With soil Cd level increasing, the SOD activity and GSH content decreased, then increased, decreased, and finally, increased; the CAT activity decreased, then increased, and eventually declined; the POD activity increased and then decreased significantly (Figure S1). The activities of SOD and CAT and GSH content were reduced by 69, 35 and 49%, respectively, in T3 (Figure S1).

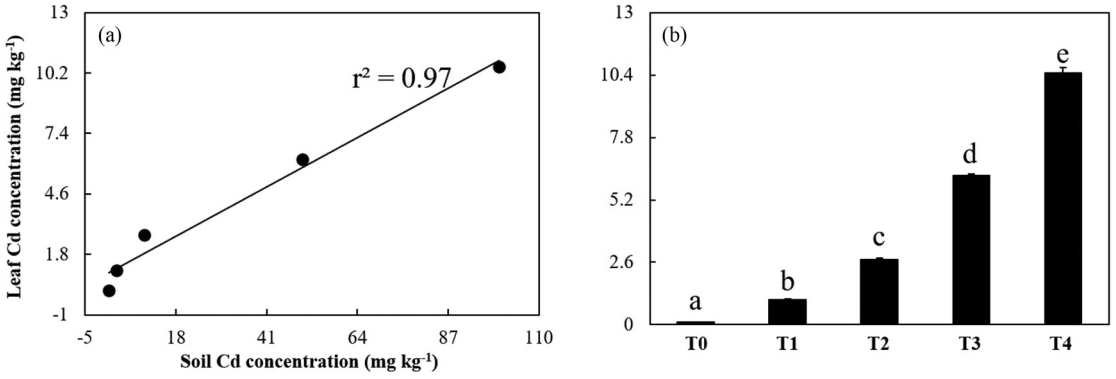

Figure 1: Enrichment characteristics of Cd in *P. asiatica* leaves with different levels of soil Cd stress; (a) stands for Cd concentration in *P. asiatica* leaves with different levels of soil Cd stress; (b) stands for relationships of leaf Cd concentration and soil Cd concentration with different levels of soil Cd stress. The data with different little letters showed significant difference; T0, T1, T2, T3, and T4 indicates samples in control, 3 mg/kg Cd stressed, 10 mg/kg Cd stressed, 50 mg/kg Cd stressed, and 100 mg/kg Cd stressed group, respectively. The data presented in mean ± SE (n = 3) (the same below).

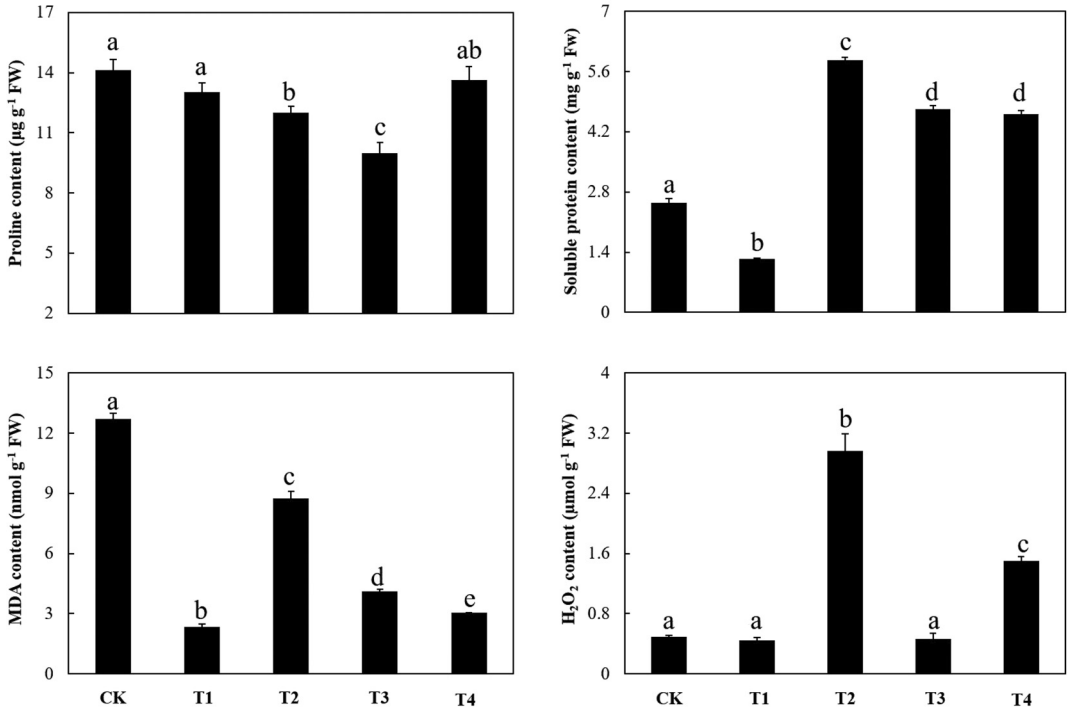

Figure 2: Contents of proline, soluble protein, MDA, and H_2O_2 in *P. asiatica* leaves with different levels of soil Cd stress. All data presented in mean ± SE (n = 3).

Besides, the Cd concentration was positively related to soluble protein content and negatively to both MDA content and activities of SOD and CAT ($p < 0.05$), and MDA content and activities of SOD and CAT showed positive relationships to each other ($p < 0.05$) (Table 1).

3.2 Top 50 DMs and top 50 DEGs in *P. asiatica*

Top 50 DMs were categorized into organic acids, sugars, alcohols, amino acids, amines, and others, with organic

Table 1: Relationships among Cd concentration, contents of soluble protein (SP), MDA, proline (Pro), H_2O_2 and GSH, and activities of SOD, POD, and CAT in *P. asiatica* leaves

r	DHA	SP	MDA	H_2O_2	SOD	CAT	POD	GSH	Pro	Cd
DHA	1.00									
SP	0.90*	1.00								
MDA	−0.94**	0.33	1.00							
H_2O_2	−0.21	0.65**	0.21	1.00						
SOD	−0.90*	−0.28	0.72**	0.02	1.00					
CAT	−0.98**	0.39	0.98**	0.24	0.69**	1.00				
POD	0.90*	0.79**	0.24	0.47	−0.42	0.25	1.00			
GSH	−0.68	0.07	0.50	0.29	0.66**	0.47	−0.16	1.00		
Pro	−0.88*	−0.38	0.14	0.12	0.61*	0.16	−0.73**	0.43	1.00	
Cd	0.92**	0.56*	−0.59*	0.41	−0.87**	−0.53*	0.50	−0.37	−0.47	1.00

Correlation coefficient (r) was obtained by Pearson correlation analysis with bivariate. *$0.1 < p < 0.05$; **$0.001 < p < 0.01$.

acids and sugars accounting for the most (Table 2). Among them, the DHA content in T3 was twice more than that in CK (Table 2; Figure S2). According to the top 50 DMs in KEGG analysis, ascorbate and aldarate metabolism, glutathione metabolism, galactose metabolism, and glyoxylate and dicarboxylate metabolism were the target metabolic pathways with $p < 0.05$ (Table 3).

Top 50 DEGs were filtered based on the p-values, as well as top 200 DEGs (Table S1). The spearman correlation analysis between the top 50 DEGs and the top 50 DMs showed that most DMs and DEGs were closely related (Figure 3; Table S2). Moreover, the target metabolic pathways were included in the common pathways (Figures S3–S6). In the network regulation diagram, which was screened based on the target metabolic pathways, L-ascorbate peroxidase (APX) was downregulated, L-gulonolactone oxidase (GULO) and DHA were upregulated, and ascorbic acid (AsA) was not detected in the study (Figure 4).

4 Discussion

4.1 Effect of Cd on physiological characteristics of *P. asiatica*

Our study revealed that Cd stress enhanced Cd residue and membrane lipid peroxidation and disrupted cellular osmotic balance in *P. asiatica* leaves, and CAT and SOD played vital roles in the Cd resistance of *P. asiatica* leaves [28].

First, MDA content reflected the degree of membrane lipid peroxidation. Soluble protein and proline were the osmoregulators, which could reflect the stress degree of heavy metals in plants [29,30]. Cd toxicity could enhance Cd concentration and the production of reactive oxygen species (ROS, e.g., H_2O_2), aggravate membrane lipid peroxidation, and disrupt osmotic balance, which resulted in the significant change for contents of H_2O_2, MDA, proline, and soluble protein [31,32], whereas antioxidant enzymes (e.g., POD, SOD, and CAT) and GSH could scavenging ROS induced by Cd stress in plant [29,30]. Hence, in this study, with soil Cd level increased, Cd concentration of *P. asiatica* leaves increased. At the same time, contents of H_2O_2, MDA, proline, and soluble protein presented significant change, for example, H_2O_2 content in T2 and T4 was higher than that in CK, proline content in T2 and T3 was lower than that in CK, soluble protein content in T2, T3, and T4 was higher than that in CK (Figure 2). The current results were inconsistent with other findings, for instance, with Cd level increasing, soluble protein content increased and then decreased markedly, contents of proline and MDA increased significantly in *Celosia cristata* [33], contents of proline, MDA and soluble protein decreased and then increased in *Quercus mongolica* [34], and contents of MDA and H_2O_2 increased in highland barley (*Hordeum vulgare*) leaves [35]. Because plant resistance abilities to Cd were affected by Cd concentration, stress time, and plant species [36], this might be caused by the differences of plant species and Cd concentrations between our study and the other studies.

Second, CAT, SOD, and soluble protein played important roles in *P. asiatica* Cd resistance, such as decreasing contents of MDA and H_2O_2. As discussed above, MDA was a reflection of the degree of membrane lipid peroxidation in plants. The higher the content, the stronger the lipid peroxidation degree. Cd stress could

Table 2: Top 50 DMs selected from all metabolites identified in *P. asiatica* leaves under Cd stress

Metabolites	RT (s)	Mass	CK (mg kg^{-1})	T3 (mg kg^{-1})	VIP	FC
Glycolic acid	5.53	147.13	0.0031 ± 0.0002	0.0044 ± 0.0002	1.12	1.39
Isobutylamine	5.72	174.17	0.0003 ± 0.0000	0.0004 ± 0.0000	1.09	1.22
1,2,4-Butanetriol	7.11	117.08	0.0006 ± 0.0000	0.0004 ± 0.0000	1.07	0.72
Glycine	7.25	174.16	0.0050 ± 0.0003	0.0082 ± 0.0005	1.14	1.64
D-Glyceric acid	7.36	147.10	0.0142 ± 0.0003	0.0161 ± 0.0002	1.13	1.14
3-Hydroxynorvaline	7.82	131.10	0.0004 ± 0.0000	0.0005 ± 0.0000	1.13	1.32
2,3-Bisphospho-glyceric acid	7.90	234.20	0.0042 ± 0.0003	0.0058 ± 0.0001	1.13	1.40
2-Hydroxybutanoic acid	8.01	117.07	0.0004 ± 0.0000	0.0003 ± 0.0000	1.09	0.66
Beta-alanine	8.07	174.16	0.0006 ± 0.0000	0.0008 ± 0.0000	1.14	1.39
Dihydroxymalonic acid	8.18	147.10	0.0048 ± 0.0001	0.0068 ± 0.0004	1.13	1.44
D-Threose	8.33	147.10	0.0115 ± 0.0002	0.0125 ± 0.0001	1.08	1.09
Butane-1,2,3,4-tetrol	8.62	147.10	0.0012 ± 0.0001	0.0006 ± 0.0001	1.09	0.52
DL-Aspartic acid	8.63	232.18	0.0004 ± 0.0001	0.0012 ± 0.0002	1.09	3.22
Gamma-aminobutyric acid	8.73	174.16	0.0287 ± 0.0007	0.0318 ± 0.0008	1.06	1.11
D-Arabinopyranose	9.60	147.10	0.0044 ± 0.0003	0.0033 ± 0.0001	1.09	0.73
Pentofuranose	9.66	147.10	0.0016 ± 0.0001	0.0012 ± 0.0001	1.11	0.76
Pentitol	9.72	147.10	0.0262 ± 0.0007	0.0224 ± 0.0002	1.13	0.86
Putrescine	9.97	174.15	0.0061 ± 0.0002	0.0051 ± 0.0002	1.10	0.84
D-Xylonate	9.98	103.07	0.0043 ± 0.0002	0.0034 ± 0.0002	1.07	0.79
Vanillic acid	10.12	207.11	0.0003 ± 0.0000	0.0002 ± 0.0000	1.13	0.63
D-Glucose 1-phosphate	10.14	217.17	0.0052 ± 0.0003	0.0031 ± 0.0003	1.13	0.60
Shikimate	10.27	204.15	0.0084 ± 0.0005	0.0056 ± 0.0004	1.12	0.67
Citrate	10.35	147.10	0.0158 ± 0.0006	0.0186 ± 0.0005	1.10	1.17
Dehydroascorbate	10.54	173.11	0.0016 ± 0.0001	0.0032 ± 0.0003	1.12	2.01
D-Tagatose	10.63	147.11	0.0054 ± 0.0002	0.0080 ± 0.0005	1.13	1.49
alpha-D-Galactose	10.77	205.43	0.0285 ± 0.0009	0.0345 ± 0.0010	1.12	1.21
beta-D-Glucose	10.87	147.14	0.0097 ± 0.0002	0.0145 ± 0.0012	1.11	1.50
D-Mannitol	10.97	206.32	0.0051 ± 0.0001	0.0058 ± 0.0002	1.10	1.16
Allose	11.00	205.28	0.0276 ± 0.0008	0.0323 ± 0.0008	1.11	1.17
alpha-D-Xylopyranose	11.18	217.19	0.0048 ± 0.0002	0.0070 ± 0.0004	1.14	1.45
D-Mannonate	11.26	147.12	0.0044 ± 0.0002	0.0052 ± 0.0001	1.12	1.19
Inositol	11.74	148.13	0.0035 ± 0.0001	0.0044 ± 0.0002	1.10	1.25
N-Acetylhexosamine	11.80	147.13	0.0077 ± 0.0001	0.0086 ± 0.0002	1.10	1.11
Phytol	12.15	143.14	0.0052 ± 0.0004	0.0036 ± 0.0001	1.12	0.68
3,7,11,15-Tetramethylhexadec-2-en-1-ol	12.15	143.14	0.0052 ± 0.0004	0.0036 ± 0.0001	1.12	0.68
L-Gulonolactone	12.19	204.18	0.0017 ± 0.0002	0.0031 ± 0.0001	1.14	1.83
4-(2-Amino-1-hydroxyethyl)benzene-1,2-diol	12.21	174.18	0.0011 ± 0.0001	0.0004 ± 0.0000	1.15	0.36
D-myo-Inositol 4-phosphate	13.16	318.25	0.0007 ± 0.0000	0.0005 ± 0.0000	1.13	0.66
L-Threo-Sphingosine C-18	13.33	204.16	0.0013 ± 0.0001	0.0010 ± 0.0000	1.07	0.75
Cytosine arabinoside monophosphate	13.35	217.17	0.0020 ± 0.0002	0.0011 ± 0.0001	1.07	0.57

(*Continued*)

Table 2: *Continued*

Metabolites	RT (s)	Mass	CK (mg kg^{-1})	T3 (mg kg^{-1})	VIP	FC
Sphingosine	13.37	204.17	0.0007 ± 0.0001	0.0005 ± 0.0000	1.06	0.69
5-Methoxytryptamine	13.39	174.16	0.0018 ± 0.0001	0.0009 ± 0.0001	1.15	0.49
Sphinganine	14.16	204.15	0.0005 ± 0.0000	0.0002 ± 0.0000	1.14	0.50
Malbit	14.55	204.15	0.0028 ± 0.0002	0.0019 ± 0.0001	1.09	0.70
beta-Lactose	14.72	204.14	0.0061 ± 0.0004	0.0047 ± 0.0004	1.05	0.76
3,4,5,6-Tetrahydroxy-2-[3,4,5-trihydroxy-6-(hydroxymethyl)oxan-2-yl]oxyhexanal	14.79	204.15	0.0063 ± 0.0004	0.0040 ± 0.0003	1.12	0.63
Disaccharide (Hex–Hex)	14.96	204.15	0.0135 ± 0.0006	0.0096 ± 0.0007	1.11	0.71
Amylotriose	15.86	361.25	0.0015 ± 0.0001	0.0024 ± 0.0002	1.09	1.61
Retinal	16.66	237.19	0.0003 ± 0.0000	0.0001 ± 0.0000	1.14	0.37
Lithocholic acid	17.85	129.09	0.0003 ± 0.0000	0.0002 ± 0.0000	1.11	0.76

The top 50 DMs were selected based on VIP value from the total DMs; CK and T3 presented samples without Cd stress and 50 mg/kg Cd stress, respectively; all data were presented in mean ± SE (n = 3); FC, ratio of metabolite content in T3 and in CK.

Table 3: Target pathways involving the top 50 DMs in *P. asiatica* leaves under Cd stress

Pathway	Total cmpd	Raw p	Rich factor	Holm adjust	FDR	Metabolites
Ascorbate and aldarate metabolism	18.00	0.01	0.17	0.57	0.55	L-Gulono-1,4-lactone; myo-Inositol; dehydroascorbate
Glutathione metabolism	26.00	0.02	0.12	1.00	0.55	Glycine; putrescine; dehydroascorbate
Galactose metabolism	27.00	0.02	0.11	1.00	0.55	Lactose; D-glucose 1-phosphate; myo-Inositol
Glyoxylate and dicarboxylate metabolism	29.00	0.02	0.10	1.00	0.55	Citrate; D-glycerate; glycine

The target metabolic pathways with pathway p value of below 0.05; Total Cmpd, total number of compounds in the pathway; Rich factor, ratio of the number of actually matched compound and total number of compound (Total Cmpd) in the pathway; Holm adjust, p value adjusted by Holm–Bonferroni method; FDR, p value adjusted using false discovery rate; metabolites in the table were involved in the target pathway.

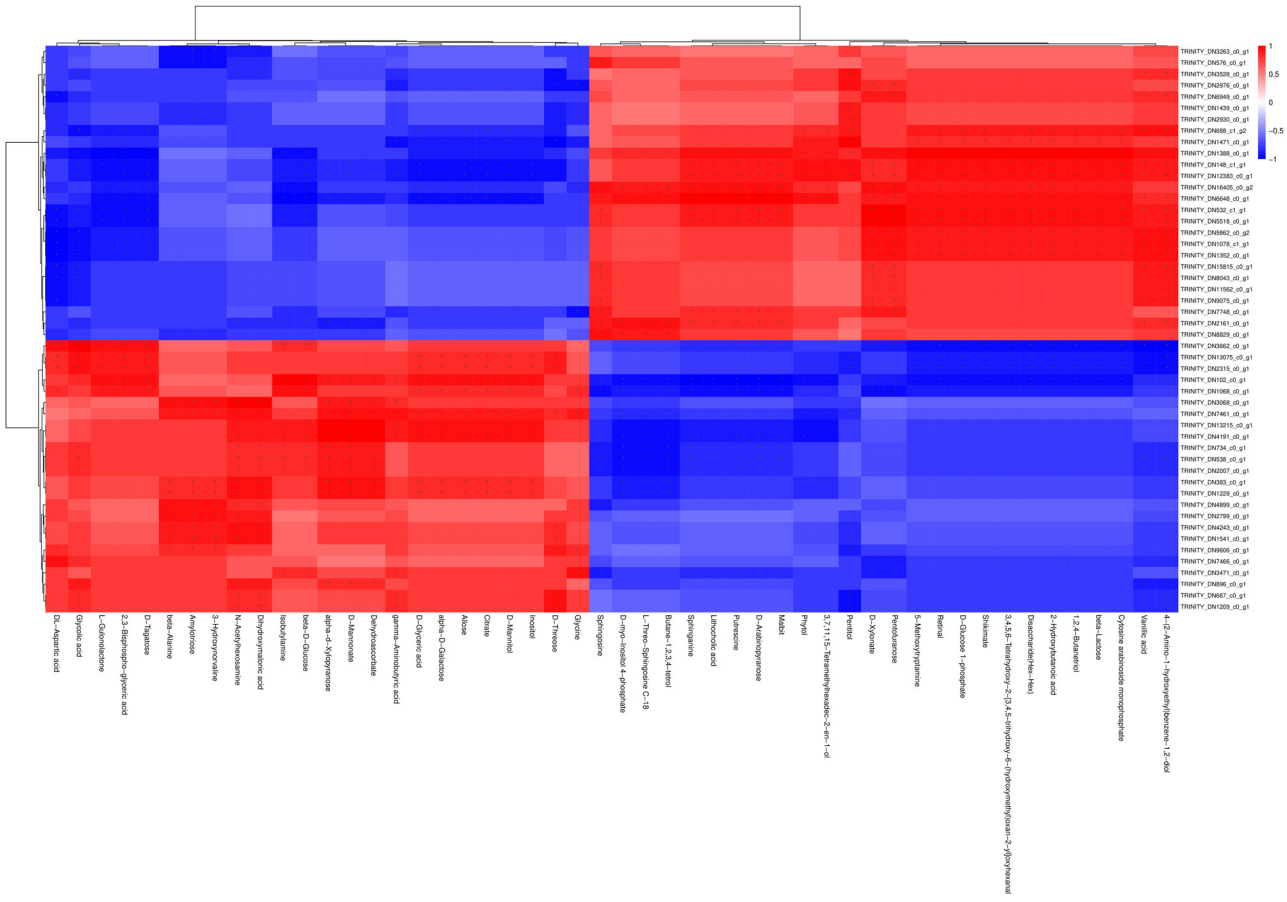

Figure 3: Correlation clustering heat map of top 50 DEGs and top 50 DMs in *P. asiatica* leaves with different levels of soil Cd stress. DMs, differential metabolites.

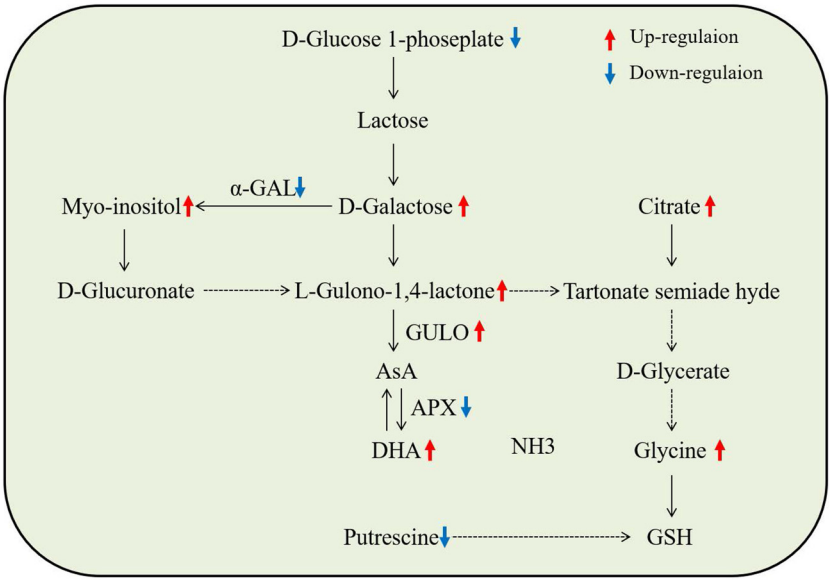

Figure 4: Metabolic network involving target metabolic pathways in *P. asiatica* leaves with different levels of soil Cd stress. α-GAL, α-galactosidase (the same below).

lead to ROS (e.g., O_2^-, OH^-, H_2O_2) enrichment and oxidative damage in the plant cell. On the one hand, SOD mainly catalyzed O_2^- to produce O_2 and H_2O_2 and CAT and POD catalyzed the decomposition of H_2O_2 to generate O_2 and H_2O. On the other hand, CAT and SOD belonged to metalloenzymes [37,38]. With soil Cd level increasing, leaf Cd concentration increased (Figure 1), CAT activity showed the same change trend with MDA content and an opposite trend of H_2O_2 content. Cd concentration showed significant correlations with MDA content and activities of SOD and CAT in leaf (Table 1). Hence, in this study, CAT might be the main catalytic enzymes in the decomposition of H_2O_2, and soluble protein played important roles in regulating intracellular osmotic potential caused by Cd stress [39]. With low Cd stress, under comprehensive function of antioxidant enzymes and GSH, MDA content decreased and soluble protein content increased, and H_2O_2 content decreased with high Cd stress to maintain the Cd resistance of *P. asiatica* [40,41]. When soil Cd level increased, metal ions of metalloenzymes (CAT and SOD) might be replaced by Cd resulting in the decline in CAT and SOD activities [38]. However, coupled with the function of POD, they also could scavenge active oxygen free radicals leading to the decline in MDA content (Figure 2) [42].

4.2 Organic acids (especially DHA) and sugars played vital roles in *P. asiatica* Cd resistance

This study showed clearly that organic acids (especially DHA) and sugars played important roles in Cd resistance in *P. asiatica* (Table 2). Heavy metal stress could affect contents of metabolites, such as organic acids and sugars (Table 2) [43–46]. Organic acids belonged to a class of compounds with carboxyl groups (excluding amino acids), most of which could chelate metal ions, and enhance plant resistance to heavy metals [43,44]. Sugars could provide sufficient energy for plants to resist heavy metal damage, and sugars were closely related to the water absorbing ability of cell, which could affect plant adaptability to Cd stress [45]. Therefore, in this study, most of the top 50 DMs belonged to organic acids and sugars (Table 2). Consistent with the results of our study, Zhang [46] found that most of the DMs between the control group and the Cd-stressed group were organic acids and sugars, which played important roles in heavy metal resistance of rice [47].

The DHA played an important role in plant resistance to abiotic stress [48] and generated from the oxidation of AsA [49], which was an important redox buffer and could remove H_2O_2 and interact directly with O_2^- and OH^- [48]. DHA coupled with oxidated AsA regulated the redox state of cells [50]. Hence, in this study, among the top 50 DMs, the relative content of DHA in *P. asiatica* leaves showed a large change in T3, which was twice more than that in CK (Table 2; Figure S2). Besides, the DHA content was positively related to Cd concentration, soluble protein content, and POD activity and negatively to MDA content and activities of SOD and CAT in leaves (Table 1). Cd toxicity enhanced the production of ROS, which damaged the cell membrane and promoted the production of MDA (Figure 2) [51]. AsA and antioxidase (e.g., SOD, CAT, and POD) worked together to convert H_2O_2 to H_2O, accompanied by the production of DHA (Table 2) [52]. In addition, soluble protein would balance the intracellular and extracellular osmotic pressure induced by Cd stress [53] (Figure 2).

4.3 GULO and APX played vital roles in *P. asiatica* Cd resistance

This study proved that GULO and APX played major roles in *P. asiatica* Cd resistance by regulating the production of DHA. First, ascorbate and aldarate metabolism, glutathione metabolism, galactose metabolism, and glyoxylate and dicarboxylate metabolism were the targeted metabolism pathways in *P. asiatica* under Cd stress (Table 3). Galactose metabolism provided energy and raw materials, e.g., D-galactose and myo-inositol, for metabolic pathways including ascorbate and aldarate metabolism, glutathione metabolism, and glyoxylate and dicarboxylate metabolism (Figure 4) [54]. As reported above, the intermediate metabolites (including AsA and GSH) of these metabolisms acted as important regulators of plant abilities of resistance to Cd [55–57]. Differing from our study, Wang et al. [54] found that the targeted metabolisms of *Zea mays* under Cd stress included tricarboxylic acid cycle metabolism, and shikimic acid metabolism. Tan et al. [56] revealed that under long-time Cd stress, the differential metabolic pathways of *Brassica juncea* included biosynthesis of amino acids, linoleic acid metabolism, aminoacyl-tRNA biosynthesis, etc. These studies have shown that different plants showed different Cd-tolerant abilities and lead to the different accumulation levels of metabolites (e.g., organic acids, amino acids, and sugars) and different targeted metabolic pathways [58].

According to KEGG analysis (Figure 3), the network regulation diagram was obtained involving the targeted metabolism pathways (Figure 4 and Figures S3–S6). In

the diagram, the relative content of DHA was regulated by APX and GULO. L-Gulono-1,4-lactone and GULO were upregulated, and APX was downregulated, while DHA was upregulated and AsA exceeded the minimum detection limit and was not detected (Figure 4; Table 2). Such observations were consistent with Jung et al. [59], and they revealed that Cd stress decreased the AsA content and increased the DHA content. In this study, APX reduced H_2O_2 to H_2O with AsA as the electron donor [49], leading to no significant change in the H_2O_2 content between the Cd-stressed group (T3) and the non-Cd-stressed group (CK) (Figure 2). This might be associated with non-observation of AsA in the present study with the GULO upregulation (Figure 4). Besides AsA was one of the antioxidant or redox metabolites in the non-enzymatic antioxidant scavenging pathway and essential for many enzymatic reactions under Cd stress [49,60–62], antioxidant enzymes (e.g., SOD, CAT, and POD) and non-enzymatic antioxidant (GSH) played comprehensive roles in the Cd resistance, So, in this study, antioxidant enzymes (e.g., SOD, CAT, and POD) and non-enzymatic antioxidant (GSH) changed significantly in T3 in comparison with CK, GSH content and activities of SOD and CAT decreased significantly, and POD activity increased significantly in T3 compared to CK (Figure S1).

5 Conclusion

Our study comprehensively revealed Cd resistance mechanisms in *P. asiatica* based on the physiological, metabolic, and transcriptomic analyses. First, as soil Cd level increased, Cd concentration increased significantly, proline content decreased and then increased significantly, and change trends of soluble protein and MDA contents were contrary to H_2O_2 content, which first increased, then declined, and finally increased ($p < 0.05$) in *P. asiatica* leaves. Leaf Cd concentration was positively related to soluble protein content and negatively to MDA content and activities of SOD and CAT ($p < 0.05$), and MDA content and activities of SOD and CAT showed positive correlations with each other ($p < 0.05$). This illuminated that CAT and SOD played important roles in Cd resistance in *P. asiatica*, and soluble protein and MDA functioned effectively in characterizing Cd damage. Second, most of the top 50 DMs were organic acids (especially DHA) and sugars. DHA content in T3 was more than twice than it in CK. Considering the important role of DHA in plant-resistant ability, this suggested that DHA might be the important substances to deal with Cd stress in *P. asiatica*. Third, ascorbate and aldarate metabolism, glutathione metabolism, galactose metabolism, and glyoxylate and dicarboxylate metabolism were the main differential metabolic pathways in *P. asiatica*. In the metabolic network, L-gulono-1,4-lactone, GULO, and DHA were upregulated, but APX was downregulated. DHA relative content was regulated by APX and GULO, so was AsA relative content. This suggested that AsA might function effectively in Cd resistance like DHA, and the functions were regulated by APX and GULO.

Funding information: This work was supported by the Scientific Research Foundation for Doctor of the Jiangxi University of Chinese Medicine [2020BSZR011] and Study on the Whole Chain Production Technology of High-quality Development of Authentic Chinese Herbal Medicine, Fructus Aurantii in Zhangshu-Genetic Mechanism and Germplasm Optimization of the High-quality Formation of Fructus Aurantii [20220346].

Author contributions: Jun Yuan and Haihui Fu designed the study and analyzed the data. Jun Yuan, Shasha Sheng, and Rongpeng Liu conducted the experiments. Jun Yuan and Xiaoyun Wang prepared and reviewed the article. All authors have read and approved the article.

Conflict of interest: Authors state no conflict of interest.

Data availability statement: Transcriptome data of *P. asiatica* under Cd stress could be downloaded from the link https://doi.org/10.6084/m9.figshare.20382201.v1. Metabolism data of *P. asiatica* under Cd stress could be downloaded from the link https://doi.org/10.6084/m9.figshare.20382120.v1. The datasets generated during and/or analyzed during the current study are available from the corresponding author on reasonable request.

References

[1] Beara IN, Lesjak MM, Jovin, EĐ, Balog KJ, Anackov GT, et al. Plantain (*Plantago* L.) species as novel sources of flavonoid antioxidants. J Agr Food Chem. 2009;57:9268–73.
[2] Najafian Y, Hamedi SS, Farshchi MK, Feyzabadi Z. Plantago major in traditional persian medicine and modern phytotherapy: a narrative review. Electron Phys. 2018;10:6390–9.
[3] Samuelsen AB. The traditional uses, chemical constituents and biological activities of *Plantago major* L.: a review. J Ethnopharmacol. 2000;71:1–21.
[4] Hong S, Oh G, Kang W, Kim O. Anticoccidial effects of the *Plantago asiatica* extract on experimental Eimeria tenella infection. Lab Anim Res. 2016;32(1):65–9.

[5] Kho MC, Park JH, Han BH, Tan R, Yoon JJ, Kim HY, et al. *Plantago asiatica* L. ameliorates puromycin aminonucleoside-induced nephrotic syndrome by suppressing inflammation and apoptosis. Nutrients. 2017;9:386.
[6] Dong C, Qin Y, Ma J, Cui W, Chen X, Hou L, et al. The active ingredients identification and antidiarrheal mechanism analysis of *Plantago asiatica* L. superfine powder. Front Pharmacol. 2021;11:612478.
[7] Commission CP. Pharmacopoeia of the people's Republic of China. Beijing: China Medical Science Press; 2015. Introduction.
[8] Yan H, Feng H, Huang W, Li H, Feng C. Evaluation for heavy metal pollution of soil and herb from the main producing area of *Salvia miltiorrhiza* Bge. in China. Chin Agric Sci Bull. 2012;28:288–93.
[9] Zhang X, Li K, Chen K, Liang J, Cui L. Effects of cadmium stress on seedlings growth and active ingredients in *Salvia miltiorrhiza*. Plant Sci J. 2013;31:583–9.
[10] Luo L. Large-scale detection and comprehensive risk assessments of multi-pesticide residues and heavy metals in medicinal plants. Beijing, China: China Academy of Chinese Medical Sciences; 2021.
[11] Kabata PA, Pendias H. Trace elements in soils and plants. Baton Rouge: CRC Press; 1992. p. 273–89.
[12] Satarug S, Baker JR, Urbenjapol S, Haswell-Elkins M, Reilly PEB, Williams DJ, et al. A global perspective on cadmium pollution and toxicity in non-occupationally exposed population. Toxicol Lett. 2003;137:65–83.
[13] Ma Q, Cao X, Tan X, Si L, Wu L. Effects of cadmium stress on pakchoi (*Brassica chinensis* L.) growth and uptake of inorganic and organic nitrogenous compounds. Env Exp Bot. 2017;137:49–57.
[14] Rizwan M, Ali S, Zia ur Rehman M, Rinklebe J, Tsang DCW, Bashir A, et al. Cadmium phytoremediation potential of Brassica crop species: a review. Sci Total Env. 2018;631–632:1175–91.
[15] Carvalho MEA, Castro PRC, Azevedo RA. Hormesis in plants under Cd exposure: From toxic to beneficial element? J Hazard Mater. 2020;384:121434.
[16] Zhang X, Zhang X, Lv S, Shi L, Wang R. Migration and transformation of cadmium in rice-soil under different nitrogen sources in polymetallic sulfide mining areas. Sci Rep. 2020;10:2418.
[17] Liu L, Wang Y, Jin Z, Zhang Z, Li S, Zhang D. Accumulation of heavy metal cadmium(II) ions by *Herba plantaginis* and its physiological responses. Heilongjiang Anim Sci Vet Med. 2016;8:15–9.
[18] Yang Y. Accumulation and subcellular distributions of copper and lead in *Herba Plantaginis*. Sichuang, China: Sichuan Agricultural University; 2010.
[19] Gong W, Dunn BL, Chen Y, Shen Y. Acclimatization of photosynthetic apparatus and antioxidant metabolism to excess soil cadmium in *Buddleja* spp. Sci Rep. 2020;10(1):21439.
[20] Hou L, Yu J, Zhao L, He X. Dark septate endophytes improve the growth and the tolerance of *Medicago sativa* and *Ammopiptanthus mongolicus* under cadmium stress. Front Microbiol. 2019;10:3061.
[21] Yuan J, Sun N, Du H, Yin S, Kang H, Umair M, et al. Roles of metabolic regulation in developing *Quercus variabilis* acorns at contrasting geologically-derived phosphorus sites in subtropical China. BMC Plant Biol. 2020;20:389.
[22] Liu R, Sheng S, Wang X, Yuan J. Characteristics of cadmium enrichment of Jiangxi daodi medicinal plant *Plantago asiatica* L. and its transcriptome analysis in response to cadmium stress. Mol Plant Breed. Forthcoming 2022. Retrieved from osf.io/preprints/socarxiv/ev4pw.
[23] Zemanová V, Pavlík M, Pavlíková D. Cadmium toxicity induced contrasting patterns of concentrations of free sarcosine, specifc amino acids and selected microelements in two Noccaea species. PLoS One. 2017;12(5):e0177963.
[24] Grabherr MG, Haas BJ, Yassour M, Levin JZ, Thompson DA, Amit I, et al. Full-length transcriptome assembly from RNA-Seq data without a reference genome. Nat Biotechnol. 2011;29:644–52.
[25] Li B, Dewey CN. RSEM: accurate transcript quantification from RNA-Seq data with or without a reference genome. BMC Bioinforma. 2011;12:323.
[26] Mao X, Cai T, Olyarchuk JG, Wei L. Automated genome annotation and pathway identification using the KEGG Orthology (KO) as a controlled vocabulary. Bioinformatics. 2005;21:3787–93.
[27] Schober P, Boer C, Schwarte LA. Correlation coefficients: appropriate use and interpretation. Anesth Analg. 2018;126:1763–8.
[28] Sardar R, Ahmed S, Ali Shah A, Ahmad, Yasin N. Selenium nanoparticles reduced cadmium uptake, regulated nutritional homeostasis and antioxidative system in *Coriandrum sativum* grown in cadmium toxic conditions. Chemosphere. 2022;287:132332.
[29] Mujahid F, Shafaqat A, Nudrat AA, Muhammad R, Farhat A, Syed AHB, et al. Phyto-management of Cr-contaminated soils by sunflower hybrids: physiological and biochemical response and metal extractability under Cr stress. Env Sci Pollut Res. 2017;24:16845–59.
[30] Szabados S, Savoure A. Proline: a multifunctional amino acid. Trends Plant Sci. 2010;15:89–97.
[31] Ali Shah A, Ahmed S, Abbas M, Ahmad Yasin N. Seed priming with 3-epibrassinolide alleviates cadmium stress in Cucumis sativus through modulation of antioxidative system and gene expression. Sci Hortic. 2020;265:109203.
[32] Ahmad A, Yasin NA, Khan WU, Akram W, Wang R, Shah AA, et al. Silicon assisted ameliorative effects of iron nanoparticles against cadmium stress: Attaining new equilibrium among physiochemical parameters, antioxidative machinery, and osmoregulators of *Phaseolus lunatus*. Plant Physiol Bioch. 2021;166:874–86.
[33] Cha Y. Preliminary study on physiological and biochemical response and Cd enrichment of *cockscomb* flower under Cd stress. Guizhou, China: Guizhou University; 2021.
[34] Zhang G. The stress effect of cadmium on *Quercus mongolica* seedlings and its alleviation by sulfur. Shenyang, China: Shenyang Agricultural University; 2020.
[35] Ren Y, Wu Y, Zhao Y, Sun S, Zhao C, Li P. Physiological comparison of leaf senescence of two highland barleys induced by cadmium stress. Mol Plant Breed. 2021. https://kns.cnki.net/kcms/detail/46.1068.S.20211018.2012.007.html.
[36] Shang YK, Liu SK, Chen YH, Liu L, Tang XB, Qin ZZ, et al. Effects of antioxidant system and soluble protein in Dongying wild soybean seedling under cadmium stress. J Sichuan Agric Univ. 2019;37(1):15–21.
[37] Bowler C. Superoxide dismutase and stress tolerance. Annu Rev Plant Phys Plant Mol Biol. 1992;43:83–116.

[38] Zhao H, Wu L, Chai T, Zhang Y, Tan J, Ma S. The effects of copper, manganese and zinc on plant growth and elemental accumulation in the manganese-hyperaccumulator *Phytolacca Americana*. J Plant Physiol. 2012;169(13):1243–52.
[39] Xie Y, Wang Y. Physiological response characteristics of four mangrove plants seedlings under heavy metal stress. J Trop Oceanograp. 2021. https://kns.cnki.net/kcms/detail/44.1500.P.20211012.1021.002.html.
[40] Lin Y, Gu X, Tang H. Characteristics and biological functions of glutathione reductase in plants. Chin J Biochem Mol Biol. 2013;29(6):534–42.
[41] Sozoniuk M, Nowak M, Dudziak K, Bulak P, Leśniowska-Nowak J, Kowalczyk K. Antioxidative system response of pedunculate oak (*Quercus robur* L.) seedlings to Cd exposure. Physiol Mol Biol Pla. 2019;25(6):1377–84.
[42] Zhang X, Wang D, Chu K, Yang C, Mou R, Chen M, et al. Changes of SOD activity and MDA content in rice exposed to Cd stress as affected by genotype. Chin J Rice Sci. 2006;20:194–8.
[43] Kuang HX. Chemistry of traditional chinese medicine. Beijing, China: China Press of Traditional Chinese Medicine; 2017.
[44] Qin M. Study on differences of metabolites in rice under cadmium stress conditions. Beijing, China: Chinese Academy of Agricultural Sciences; 2018.
[45] Yan S, Su W, Sun W. Proteomic analysis of salt stress responsive proteins in rice root. Proteomics. 2005;5:235–44.
[46] Zhang Y. Effects of cadmium on physiology, biochemistry and metabonomics of different rice varieties. Tianjin, China: Tianjin Agricultural University; 2021.
[47] Wang J. Metabolomic responses of rice seedlings to elevated CO_2 concentration and/or Pb stress Shenyang. China: Shenyang Normal University; 2020.
[48] Wells W, Xu D. Dehydroascorbate reduction. J Bioenerg Biomembr. 1994;26(4):369–77.
[49] Hasanuzzaman M, Hossain MA, da Silva JAT, Fujita M. Plant responses and tolerance to abiotic oxidative stress: Antioxidant defense is a key factor. In: Venkateswarlu B, Shanker A, Shanker C, Maheswari M, editors. Crop stress and its management: perspectives and strategies. Dordrecht: Springer; 2012. p. 261–315.
[50] Pastori G, Foyer C. Common components, networks, and pathways of cross-tolerance to stress. The central role of "redox" and abscisic acid-mediated controls. Plant Physiol. 2002;129:460–8.
[51] Soleimani M, Hajabbasi MA, Afyuni M, Mirlohi A, Borggaard OK, Holm PE. Effect of endophytic fungi on cadmium tolerance and bioaccumulation by *Festuca Arundinacea* and *Festuca Pratensis*. Int J Phytoremediat. 2010;12:535–49.
[52] Hu S, Hu B, Chen Z, Vosátka M, Vymazal J. Antioxidant response in arbuscular mycorrhizal fungi inoculated wetland plant under Cr stress. Env Res. 2020;191:110203.
[53] Zhao H, Tang J, Zheng W. Effects of Cu^{2+} stress on the growth and some physiological characteristics of mangrove *Kandelia obovate*. Mar Sci. 2016;40(4):65–72.
[54] Wang R, Lin K, Chen H, Qi Z, Liu B, Cao F, et al. Metabolome analysis revealed the mechanism of exogenous glutathione to alleviate cadmium stress in maize (*Zea mays* L.) seedlings. Plants. 2021;10:105.
[55] Dorion S, Ouellet GC, Rivoal J. Glutathione metabolism in plants under stress: beyond reactive oxygen species detoxification. Metabolites. 2021;11(9):641.
[56] Tan P, Zeng C, Wan C, Liu Z, Dong X, Peng J, et al. Metabolic profiles of *Brassica juncea* roots in response to cadmium stress. Metabolites. 2021;11(6):383.
[57] Iannelli MA, Pietrini F, Fiore L, Petrilli L, Massacci A. Antioxidant response to cadmium in *Phragmites australis* plants. Plant Physiol Bioch. 2002;40:977–82.
[58] Xie Y, Hu LX, Du ZM, Sun XY, Amombo E, Fan JB, et al. Effects of cadmium exposure on growth and metabolic profile of bermudagrass [*Cynodon dactylon* (L.) Pers.]. PLoS One. 2014;9:e115279.
[59] Jung H, Lee B, Chae M, Lee E, Lee T, Jung G, et al. Ascorbate-mediated modulation of cadmium stress responses: reactive oxygen species and redox status in *Brassica napus*. Front Plant Sci. 2020;11:5865547.
[60] Gill SS, Tuteja N. Reactive oxygen species and antioxidant machinery in abiotic stress tolerance in crop plants. Plant Physiol Bioch. 2010;48:909–30.
[61] Sharma S, Anand G, Singh N, Kapoor R. Arbuscular mycorrhiza augments arsenic tolerance in wheat (*Triticum aestivum* L.) by strengthening antioxidant defense system and thiol metabolism. Front Plant Sci. 2017;8:906.
[62] Yan H, Filardo F, Hu X, Zhao X, Fu D. Cadmium stress alters the redox reaction and hormone balance in oilseed rape (*Brassica napus* L.) leaves. Env Sci Pollut Res. 2015;23:3758–69.